Diagnostic Value of ^{18}F-FDG PET/CT Versus MRI in the Setting of Antibody-Specific Autoimmune Encephalitis

Lilja B. Solnes[1], Krystyna M. Jones[1], Steven P. Rowe[1], Puskar Pattanayak[1], Abhinav Nalluri[2], Arun Venkatesan[2], John C. Probasco[2], and Mehrbod S. Javadi[1]

[1]The Russell H. Morgan Department of Radiology and Radiological Science, Johns Hopkins University School of Medicine, Baltimore, Maryland; and [2]The Department of Neurology, Johns Hopkins University School of Medicine, Baltimore, Maryland

Diagnosis of autoimmune encephalitis presents some challenges in the clinical setting because of varied clinical presentations and delay in obtaining antibody panel results. We examined the role of neuroimaging in the setting of autoimmune encephalitides, comparing the utility of ^{18}F-FDG PET/CT versus conventional brain imaging with MRI. **Methods:** A retrospective study was performed assessing the positivity rate of MRI versus ^{18}F-FDG PET/CT during the initial workup of 23 patients proven to have antibody-positive autoimmune encephalitis. ^{18}F-FDG PET/CT studies were analyzed both qualitatively and semiquantitatively. Areas of cortical lobar hypo (hyper)-metabolism in the cerebrum that were 2 SDx from the mean were recorded as abnormal. **Results:** On visual inspection, all patients were identified as having an abnormal pattern of ^{18}F-FDG uptake. In semiquantitative analysis, at least 1 region of interest with metabolic change was identified in 22 of 23 (95.6%) patients using a discriminating *z* score of 2. Overall, ^{18}F-FDG PET/CT was more often abnormal during the diagnostic period than MRI (10/23, 43% of patients). The predominant finding on brain ^{18}F-FDG PET/CT imaging was lobar hypometabolism, being observed in 21 of 23 (91.3%) patients. Hypometabolism was most commonly observed in the parietal lobe followed by the occipital lobe. An entire subset of antibody-positive patients, anti–*N*-methyl-D-aspartate receptor (5 patients), had normal MRI results and abnormal ^{18}F-FDG PET/CT findings whereas the other subsets demonstrated a greater heterogeneity. **Conclusion:** Brain ^{18}F-FDG PET/CT may play a significant role in the initial evaluation of patients with clinically suspected antibody-mediated autoimmune encephalitis. Given that it is more often abnormal when compared with MRI in the acute setting, this molecular imaging technique may be better positioned as an early biomarker of disease so that treatment may be initiated earlier, resulting in improved patient outcomes.

Key Words: ^{18}F-FDG PET/CT; autoimmune encephalitis; altered mental status; antibody specific encephalitis; MRI

J Nucl Med 2017; 58:1307–1313
DOI: 10.2967/jnumed.116.184333

Accurate diagnosis of autoimmune encephalitis (AE) can be difficult in the clinical setting because of clinical symptoms and laboratory findings that overlap with other encephalitides. The clinical symptoms are varied and include seizures, rapid cognitive decline, and movement disorders. A subset of these autoimmune encephalitides is associated with detectable autoantibodies targeting neuronal cell antigens, some of which are paraneoplastic because they occur in the setting of cancer or cancer recurrence (*1–3*). Previous studies have shown that autoantibodies targeting cell surface proteins, such as the anti–*N*-methyl-D-aspartate receptor (anti-NMDAR), can directly disrupt the normal function of affected neurons (*4,5*).

The most well-characterized autoantibody-mediated AE in the nuclear medicine literature is anti-NMDAR encephalitis (*6,7*). Patients with anti-NMDAR encephalitis tend to be young women, and a subset of these are paraneoplastic, most commonly in the setting of ovarian teratomas (*8–10*). The predominant initial clinical symptoms are personality and behavioral changes, followed by short-term memory loss, movement disorders, seizures, and decline in level of consciousness and central hypoventilation (*7,11*). Conventional workup includes clinical history, autoantibody testing, cerebrospinal fluid (CSF) sampling, electroencephalography, and MRI (*12,13*). First-line therapies include steroids, intravenous immunoglobulins, or plasmapheresis whereas second-line therapies include rituximab and cyclophosphamide (*14*). Surgical removal of ovarian teratomas (when present) has been shown to improve clinical outcome (*15*). Delay in the initiation of therapy has been shown to result in poor outcomes for patients (*16*).

Extrapolating from the clinical experience in anti-NMDAR and other forms of seropostive AE, a variety of diagnostic studies are used in the diagnosis of suspected AE. CSF sampling may demonstrate evidence of intrathecal inflammation, whereas electroencephalography may demonstrate findings ranging from focal slowing to status epilepticus. Serum and CSF autoantibody assays are performed to detect known associated autoantibodies for diagnosis, prognostication, and guidance in occult malignancy evaluation, and to inform immunotherapy regimen selection. However, because of a prolonged time for autoantibody assay results to return and the possibility of a commercial autoantibody assay being normal with no autoantibody detected, immunotherapy must often be instituted on the basis of clinical presentation and paraclinical findings available in the interim (*17,18*). This has prompted investigation into biomarkers that may further aid in the early diagnosis of AE.

Along with CSF analysis, electroencephalogram, and clinical examination, imaging is included in the workup of suspected AEs. The most common imaging technique used is MRI of the brain. If findings are present on MRI, they are most frequently T2/fluid-attenuated inversion recovery (FLAIR) hyperintensities involving the hippocampi that may be unilateral or bilateral. These hyperintensities may extend into the thalami, striatum, brain stem, or cerebellar

Received Sep. 16, 2016; revision accepted Jan. 5, 2017.
For correspondence or reprints contact: Lilja B. Solnes, The Russell H. Morgan Department of Radiology and Radiological Science, Johns Hopkins University School of Medicine, 601 N. Caroline St., Baltimore, MD 21287.
Published online Feb. 16, 2017.

peduncles (*19*). Enhancement is variable. Traditionally, ^{18}F-FDG PET/CT has been used to assess for occult malignancy as a cause for encephalitis. Recent publications have begun to explore the added value of brain ^{18}F-FDG PET/CT in evaluating these patients (*18,20–22*). Several groups have suggested that ^{18}F-FDG PET/CT may be used to evaluate the efficacy of therapy (*20,23*). This study explores the utility of ^{18}F-FDG PET/CT as a biomarker for definite, seropositive AE and its utility when compared with conventional anatomic imaging with MRI.

MATERIALS AND METHODS

Patient Selection

This retrospective analysis was approved by our hospital's institutional review board. The electronic medical record and administrative databases at our institution were queried for neurology in-patients who had been diagnosed with AE from 2006 to 2015. Diagnosis of definite AE was based on consensus clinical criteria (*17*). Twenty-three patients with seropositive AE were identified. Patients who underwent a resting ^{18}F-FDG PET/CT and an MRI of the brain during the diagnostic period were selected. Basic patient demographic and clinical information including age, sex, symptoms at presentation, duration of symptoms before admission and imaging studies, and antibody status were recorded. For continuous variables, median and interquartile ranges are presented whereas numbers and proportions are presented for categoric variables.

Antibody Panel

A sample of the patients' blood or CSF had been drawn and submitted for autoantibody analysis in all patients. This was performed as standard of care during the patient's initial workup. Positive autoantibody panels were recorded for each patient.

Brain ^{18}F-FDG PET/CT

Resting brain ^{18}F-FDG PET/CT images were acquired in 3-dimensional (3D) mode for 10 min on a Discovery DRX or DLS (GE Healthcare; 20 patients) or a Biograph mCT (Siemens; 3 patients) with in-line CT for attenuation correction. Images were reconstructed by both filtered backprojection and ordered-subset expectation maximization methods. Activity in each voxel was normalized to the pons. The qualitative and semiquantitative analysis of the brain ^{18}F-FDG PET/CT images were independently assessed by 2 board-certified nuclear radiologists. The qualitative interpretation was based on a visual assessment of ^{18}F-FDG uptake, and each scan was scored as normal or abnormal by consensus.

After stereotactic anatomic standardization, ^{18}F-FDG activity was projected to predefined surface pixels (3D stereotactic surface projections). Three-dimensional stereotactic surface projections allow surface-rendered displays in addition to the axial, sagittal, and coronal images. The brain maps were compared with a commercially available normal database, which was also normalized to the pons (Cortex ID; GE Healthcare). Automated voxel-by-voxel z scores generated by Cortex ID (using age-matched control subjects whenever possible) were calculated for the following regions of interest: parietal cortex, frontal cortex, temporal cortex, occipital cortex (z score = [mean database − mean subject]/SD database).

The average z scores display the magnitude of metabolic change for each region with voxel-based color coding. In semiquantitative analysis, a z score threshold of greater than 2 (≃ 1.96 2-tail) corresponding to a P value of 0.05 (2-tail) was applied for demarcation of significant abnormalities; positive z scores indicate hypometabolism. All values were also validated by visual inspection.

A range of different thresholds was previously suggested for the diagnosis of dementia of Alzheimer disease on brain ^{18}F-FDG PET/CT (*24,25*). However, there is no predetermined validated cutoff point for a z score in the setting of AE. Therefore, we performed a sensitivity analysis to determine how redefining the z score threshold changes the observed outcome (*26*). We examined the number of patients with abnormal cortical metabolism using different discriminating thresholds of z scores greater than 1.64 (2-tail $P = 0.1$) and z score greater than 2.58 (2-tail $P = 0.01$).

MRI Brain

All MRI studies incorporated standard brain protocol sequences including FLAIR, T2, T1, diffusion-weighted imaging, and in some cases contrast-enhanced T1-weighted sequences. In addition to review of the radiologic report at the time of acquisition, images were reviewed by a radiologist with subspecialty neuroradiology training for imaging findings suggestive of encephalitis. MR images without evidence of underlying encephalitis or inflammatory changes were recorded as negative whereas those with findings suggestive of the above etiologies were considered positive. Chronic findings such as microvascular changes and atrophy were considered negative for the purposes of this study.

RESULTS

Patient Population

Twenty-three patients with seropositive AE were included (14 men, 9 women; median age, 46 y). The clinical characteristics of the included patients are summarized in Table 1. All patients presented with either altered mentation or impaired working memory whereas 21 (87%) presented with new focal neurologic deficits and 13 (52%) presented with seizures. Brain ^{18}F-FDG PET/CT was performed before the initiation of treatment (6 patients) or after initiation of steroid therapy (8 patients), intravenous immunoglobulins, and steroid therapy (2 patients); antibiotic and steroid therapy (1 patient); benzodiazepine therapy (3 patients); plasmapheresis (1 patient); plasmapheresis and steroid therapy (1 patient); or cellcept (1 patient).

Antibody Results

Autoantibody assay results included positive tests for anti-VGKC complex (6 patients), anti-NMDAR (5 patients), antiglutamic acid decarboxylase (anti-GAD65) (3 patients), anti-Hu (3 patients), anti-Ma (2 patients), antileucine-rich glioma-inactivated 1 (2 patients), and anti–alpha-3 acetylcholine receptor (2 patients) antibodies. Most of these were detected in the serum. CSF samples for 5 patients were tested for the presence of autoantibodies, with an autoantibody detected in only 1 patient (anti-NMDAR, patient 1) who was seronegative in the serum. The number of patients with each antibody profile within this cohort is listed in Table 2. Of note, 4 of 10 (40%) women were anti-NMDAR seropositive.

Imaging Findings

Twenty-three brain ^{18}F-FDG PET/CT scans were obtained in 23 patients with detectable autoantibodies. The duration of symptoms before PET scanning was a median of 8 wk (interquartile range, 11). All ^{18}F-FDG PET/CT scans but 2 underwent a concurrent (within 2 wk) MRI scan (Table 1). The median time between ^{18}F-FDG PET/CT scanning and brain MR imaging was 3 d (interquartile range, 7). The results of visual and semiquantitative interpretation of cortical ^{18}F-FDG PET/CT in comparison to MRI is shown in Table 2.

On visual inspection, all patients were identified to have an abnormal pattern of ^{18}F-FDG uptake. Semiquantitative analysis revealed significant metabolic change in at least 1 cortical region of interest in 22 of 23 (95.6%) of patients (z score > 2). The predominant finding on brain ^{18}F-FDG PET/CT imaging was lobar hypometabolism (Fig. 1), being observed in 21 of 23 (91.3%)

TABLE 1
Clinical Characteristics of Patients Included in Study

Patient no.	Age (y)	Sex	Altered mental status or working memory deficit	New focal neurologic findings	Seizure	Duration of symptoms before presentation (wk)	Duration of symptom onset to ^{18}F-FDG PET/CT (wk)	Duration between MRI and ^{18}F-FDG PET/CT (d)	Type of ^{18}F-FDG PET/CT scanner
1	33	F	Yes	Yes	Yes	2	2	2	GE RX
2	20	F	Yes	Yes	Yes	3	3	13	GE RX
3	57	F	Yes	Yes	Yes	12	12	6	GE RX
4	21	F	Yes	Yes	Yes	1	1	1	GE RX
5	7	M	Yes	Yes	Yes	1	1	24	GE RX
6	67	M	Yes	Yes	Yes	8	8	11	GE RX
7	59	M	Yes	Yes	No	4	4	10	GE LS
8	66	F	Yes	Yes	No	16	16	3	GE RX
9	65	M	Yes	No	Yes	8	8	0	GE RX
10	43	M	Yes	Yes	Yes	12	12	1	GE LS
11	70	M	Yes	Yes	No	1	0	3	GE RX
12	50	F	Yes	Yes	Yes	4	36	4	Siemens
13	33	M	Yes	No	No	0	0	7	GE RX
14	62	M	Yes	Yes	No	8	8	3	GE RX
15	18	F	Yes	Yes	Yes	0	0	2	GE RX
16	76	M	Yes	Yes	No	1	1	7	GE LS
17	61	M	Yes	Yes	No	8	8	1	Siemens
18	67	M	Yes	Yes	No	1	1	1	GE RX
19	22	F	Yes	Yes	Yes	8	8	7	GE RX
20	40	M	Yes	Yes	Yes	4	24	4	GE RX
21	72	F	Yes	Yes	No	5	12	1	GE LS
22	9	M	Yes	No	No	16	20	32	GE RX
23	46	M	Yes	Yes	No	4	4	0	Siemens

patients. Findings suggestive of encephalitis on MRI were seen in 10 of 23 (43%) patients. The most common positive MRI finding in patients was increased T2/FLAIR signal in the medial temporal lobes (Fig. 2). A single case (patient 6) was identified as abnormal on visual inspection but normal by *z* score measures. The visual assessment identified a small area of increased tracer uptake in the medial right frontal lobe. This focus was likely not large enough to render an abnormal semiquantitative measure on the *z* score map. This finding underscores the importance of primary visual assessment of each scan.

The *z* scores demonstrating a hypometabolic pattern are shown in Figure 3 (regions sorted by median *z* scores in descending order). Hypometabolism was most pronounced in the parietal lobe followed by the occipital lobe, with a median *z* score of 2.62 and 2.32, respectively.

As determined by Cortex ID, 19 of 23 (82.6%) scans demonstrated abnormal metabolic activity (hyper or hypo) in a parietal lobe distribution. This finding was often bilateral (15/19, 78.9%). The temporal lobes were least affected by metabolic change, with 12 of 23 (52.2%) scans demonstrating metabolic abnormalities. The metabolic change was bilateral in most temporal abnormality cases (6/12, 50%). In semiquantitative analysis, at least 1 lobar region with metabolic change was identified in 23 of 23 (100%), 22 of 23 (95.6%), and 20 of 23 (86.9%) patients using discriminating *z* scores of 1.64, 2.0, and 2.58, respectively.

Discrepancy in ^{18}F-FDG abnormality and MRI findings was most pronounced in the setting of patients with anti-NMDAR antibodies. None of these patients demonstrated abnormal MRI findings whereas all 5 demonstrated a significantly abnormal ^{18}F-FDG PET/CT scan result. A characteristic wedge-shaped hypometabolic defect was seen in the occipital lobes in patients with anti-NMDAR (Fig. 4). Both anti-alpha3 acetylcholine receptor patients had abnormal ^{18}F-FDG PET/CT findings but a normal MRI scan. Patients with anti-VGKC seropositivity were more likely to have a concordant abnormal MRI than not (80% [4/5] in semiquantitative PET assessment and 66.7% [4/6] in visual PET assessment).

DISCUSSION

Early diagnosis is paramount for patients with AE because it can inform earlier treatment, which may improve outcomes (*27*). Diagnosis is dependent not only on autoantibody testing and response to immunotherapy but also on clinical presentation and other paraclinical findings (*28*). Depending on autoantibody, testing to make the diagnosis may significantly delay treatment initiation. Moreover,

TABLE 2
Imaging Findings of Patients Included in Study

Patient no.	Antibody	^{18}F-FDG PET/CT result				Brain MRI interpretation
			Semiquantitative analysis (3D-SSP)*			
		Visual PET interpretation	Cortical regions with significant metabolic change		Interpretation	
			Hypometabolism	Hypermetabolism		
1	Anti-NMDA	Abnormal	**PAR (R,** L), TMP (R), **FRT (R,** L), **OCC (R, L)**	—	Abnormal	Normal
2	Anti-NMDA	Abnormal	**PAR (R, L), TMP (R,** L), **FRT (R, L), OCC (R, L)**	—	Abnormal	Normal
3	Anti-NMDA	Abnormal	**PAR (R, L),** FRT (R, L), **OCC (R, L)**	—	Abnormal	Normal
4	Anti-NMDA	Abnormal	OCC (R)	—	Abnormal	Normal
5	Anti-NMDA	Abnormal	**PAR (L), OCC (R, L)**	—	Abnormal	Normal
6	Anti-VGKC	Abnormal	—	—	Normal	Normal
7	Anti-VGKC	Abnormal	PAR (R**, L)**, TMP (L), FRT (R, L), OCC (L)	—	Abnormal	Abnormal
8	Anti-VGKC	Abnormal	**PAR (R,** L), FRT (R), OCC (R, L)	—	Abnormal	Normal
9	Anti-VGKC	Abnormal	**PAR (R, L),** TMP (R, L), **FRT (R, L), OCC (R, L)**	—	Abnormal	Abnormal
10	Anti-VGKC	Abnormal	PAR (R, L), TMP (R), FRT (R, L)	—	Abnormal	Abnormal
11	Anti-VGKC	Abnormal	**PAR (L)**	**TMP (R),** FRT (R), OCC (R)	Abnormal	Abnormal
12	Anti-Ma2	Abnormal	PAR (L), TMP (L), **FRT (L), OCC** (R, **L)**	—	Abnormal	Abnormal
13	Anti-Ma2	Abnormal	**PAR (R, L), TMP (R, L), FRT (R, L), OCC** (R**, L)**	—	Abnormal	Abnormal
14	Anti-Hu	Abnormal	**PAR (R,** L), FRT (R, L), **OCC** (R, **L)**	—	Abnormal	Normal
15	Anti-Hu	Abnormal	—	**PAR (R, L),** TMP (R, L), FRT (R, L), **OCC** (R, **L)**	Abnormal	Abnormal
16	Anti-Hu	Abnormal	FRT (R, L), OCC (R)	—	Abnormal	Normal
17	Anti-LGI1	Abnormal	**PAR (R, L),** TMP (R, L), FRT (R, L), OCC (R, L)	—	Abnormal	Normal
18	Anti-LGI1	Abnormal	PAR (R), TMP (R), FRT (R, L), OCC (R, L)	—	Abnormal	Abnormal
19	Anti-GAD65	Abnormal	PAR (R, L), FRT (R)	—	Abnormal	Abnormal
20	Anti-GAD65	Abnormal	**PAR (R, L)**, FRT (R, L), OCC (L)	—	Abnormal	Normal
21	Anti-GAD65	Abnormal	**PAR (R,** L), OCC (R)	—	Abnormal	Abnormal
22	Antiialpha3ACHR	Abnormal	OCC (R**, L)**	—	Abnormal	Normal
23	Anti-alpha3ACHR	Abnormal	**PAR (R, L),** TMP (R, L), FRT (R, L), OCC (L)	—	Abnormal	Normal

*Average z score > 2 (2-tail $P = 0.05$) was considered as significant metabolic change. Bold regions represent areas with higher absolute z scores (absolute $z > 2.58$, 2-tail $P = 0.01$).

3D-SSP = 3D stereotactic surface projections; PAR = parietal cortex; TMP = temporal lobe; OCC = occipital lobe; FRT = frontal lobe.

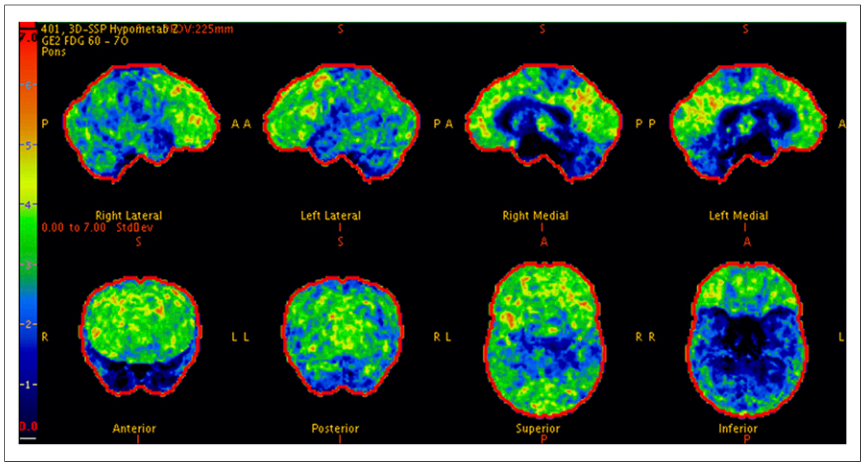

FIGURE 1. A 65-y-old man presenting with confusion, seizures, and hyponatremia. Paraneoplastic panel was positive for voltage-gated potassium channel autoantibodies. Brain ^{18}F-FDG PET *z* score maps demonstrate significant supratentorial cerebral hypometabolism relative to cerebellar metabolic activity. Color bar represents scale of *z* scores.

autoantibody testing is not readily available at many institutions and can take several weeks to obtain. Recently, leading authorities on the diagnosis and treatment of AE convened and recommended criteria for the diagnoses of possible, probable, and definite AE to mitigate the delay in initiation of therapy while awaiting autoantibody assay results (*17*). The parameters described in the report included clinical symptoms, CSF sampling, serum sampling, electroencephalogram findings, and MRI. The panel did not include ^{18}F-FDG PET/CT in their recommendations in the diagnosis of possible AE or seronegative probable AE. This is despite reports that have described characteristic findings that support the value of ^{18}F-FDG PET/CT in the diagnostic workup of AE (*29–33*). PET imaging was likely not included because more work is needed to delineate the exact role of this molecular imaging technique in the setting of suspected AE as well as patterns characteristic of the various AE syndromes.

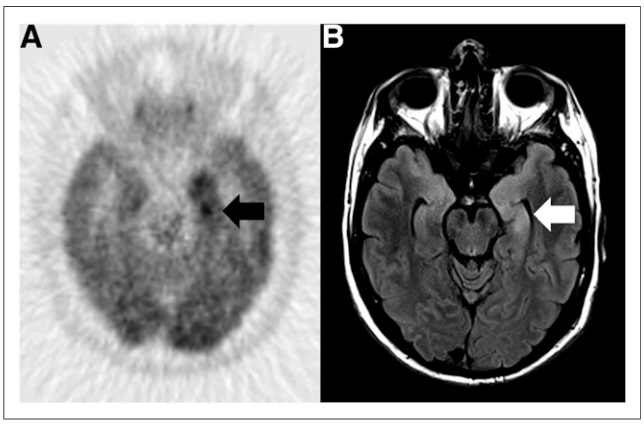

FIGURE 2. A 59-y-old man with 3-mo history of progressive memory and cognitive difficulties. Paraneoplastic panel was positive for voltage-gated potassium channel autoantibodies. Axial 3D ^{18}F-FDG PET/CT image (A) demonstrates intense ^{18}F-FDG uptake (black arrow) at medial temporal lobe (left side greater than right side). Axial T2 FLAIR MRI (B) shows abnormal signal (white arrow) within same regions. Semiquantitative analysis revealed significant change in brain metabolism in bilateral frontal (*z* scores of 2.14 [right] and 2.3 [left]), bilateral parietal (*z* scores of 2.55 [right] and 2.88 [left]), left temporal (*z* score of 2.03), and left occipital lobes (*z* score of 2.18).

In this study, we found that brain ^{18}F-FDG PET/CT was much more likely to be abnormal than MRI of the brain. The predominant PET abnormality in our study is a pattern of lobar hypometabolism involving the cerebral cortices. Previously, Clapp et al. evaluated brain metabolism with ^{18}F-FDG PET in patients with paraneoplastic neurologic syndromes. They have shown that most patients with diffuse cerebral hypometabolism had clinical syndromes consistent with encephalitis (72.2% patients) (*34*). However, a heterogeneous pattern of brain metabolism has been reported on the brain ^{18}F-FDG PET/CT of patients with AE so far (*34–38*). Some previous case reports described hypermetabolism of cerebral cortices or striatum as a predominant feature of autoimmune encephalitides (*35,37–39*). This may in part be due to the fact that we are measuring the metabolic activity of entire lobes/predetermined regions by Cortex ID. When visually examining these studies, there may be small foci of relatively increased activity with global decrease of lobar cortical metabolic activity. A small number of our patients demonstrated increased metabolic activity in the caudate nuclei (unilateral or bilateral). The implications of this finding need further investigation in a larger cohort of patients without clinical symptoms of encephalitis.

In our study, 56.5% (13/23) patients with abnormal ^{18}F-FDG PET/CT results had no abnormal finding on MRI, suggesting the limited sensitivity of MRI in AE. This study suggests that ^{18}F-FDG PET/CT imaging may serve as an early biomarker to capture more patients in the initial clinical evaluation process of AE. More work needs to be done to determine whether there are patterns of abnormal cortical metabolic activity that distinguish seropositive from seronegative AE. Among the seropositive group, we saw distinct autoantibody-specific patterns of abnormal uptake among certain subgroups. For example, in the anti-NMDAR subgroup there was profound hypometabolism of the visual cortices at diagnosis. This finding was not associated with any changes on visual examination or reported visual symptoms. Consistent with our study, some previous brain ^{18}F-FDG PET/CT studies on patients with anti-NMDAR limbic encephalitis have demonstrated metabolic abnormalities in different brain areas including hypometabolism in the cortical areas and thalamus, sometimes accompanied by hypermetabolism in the striatum (*36*). In our subset of patients, none of the anti–NMDAR-positive patients demonstrated findings on MRI suggestive of encephalitis. Hence, brain ^{18}F-FDG PET/CT rather than MRI may be indicated in the workup of young women thought to have anti-NMDAR encephalitis (*29,36*).

As noted before, several antibodies have been found to cause AE. These autoantibodies may target intracellular proteins (e.g., Hu and Ma-2) and serve as markers of autoimmunity rather than play a pathogenic role, whereas others are thought to target cell surface proteins (e.g., leucine-rich glioma-inactivated 1, NMDAR) and play an important role in syndrome pathogenesis (*2,40–42*). Some of these autoantibodies are thought to be paraneoplastic, particularly those targeting intracellular proteins. For example, Hu and Ma2 syndromes are often present in the setting of neoplasia (*43–45*). However, our results did not demonstrate a significant relationship between the presence of neoplasia and abnormal brain ^{18}F-FDG PET/CT findings, and

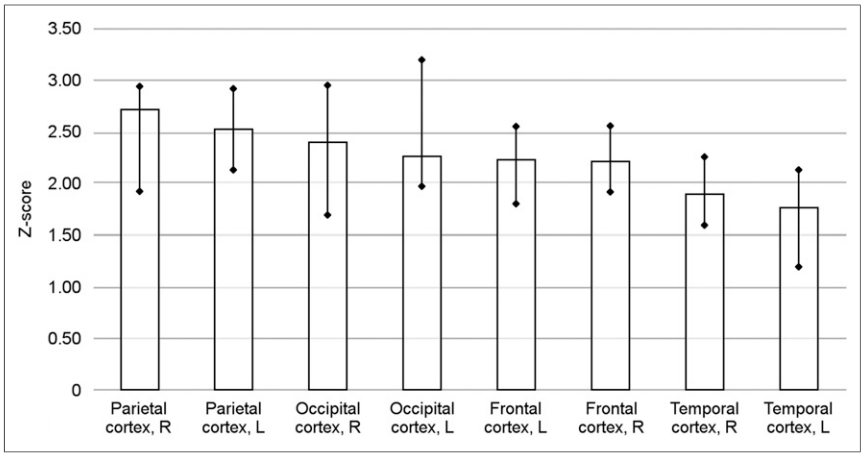

FIGURE 3. Region-of-interest analysis; *z* scores of hypometabolic pattern in AE. Histograms represent median values, and error bars refer to interquartile ranges. Regions sorted by median *z* scores in descending order.

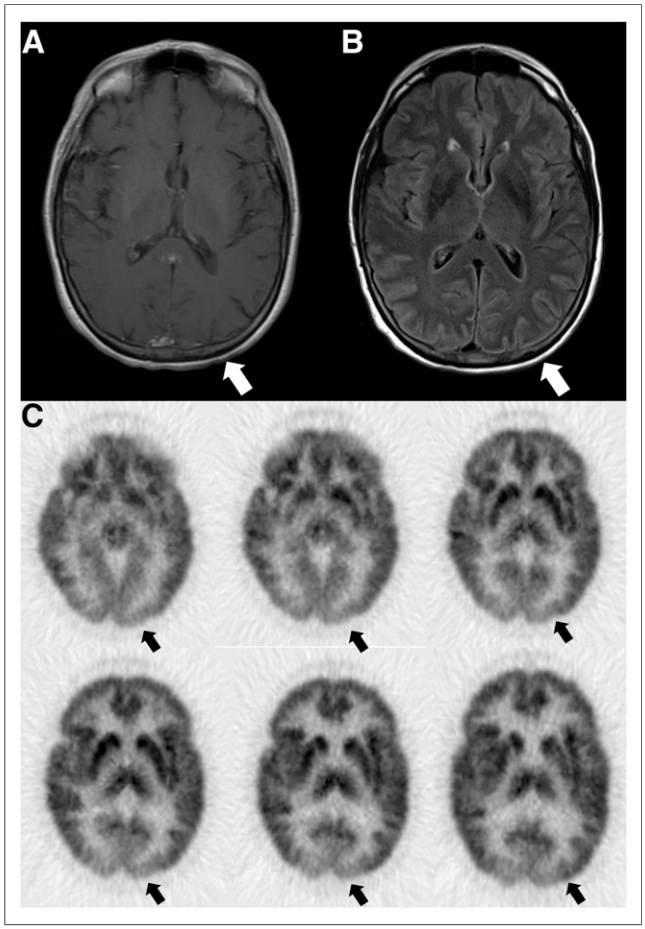

FIGURE 4. A 57-y-old woman presenting with catatonia and psychosis found to have paraneoplastic limbic encephalitis. Paraneoplastic panel was positive for anti-NMDAR. Post–contrast-enhanced T1-weighted (A) and T2 FLAIR (B) MRI at level of occipital lobes shows no evidence of any abnormality (white arrows). Axial images of ^{18}F-FDG PET/CT (C) reveal regions of significant hypometabolism in bilateral visual cortices (*z* score $>$ 2).

thus brain ^{18}F-FDG PET/CT may serve as a useful biomarker for both paraneoplastic and nonparaneoplastic populations. A caveat is the relatively small sample size of our group, and thus larger population studies are required for further characterization.

To the best of our knowledge, this study presents the largest cohort of patients with proven antibody-positive AE who underwent both brain ^{18}F-FDG PET/CT and MRI. Nevertheless, the small sample size particularly limits the conclusions that can be drawn on the basis of our subgroup analysis. Some other limitations of our study include its retrospective nature, the long lag time between the scan and clinical presentation, and variation in treatment status. Studied cases were identified via key words and diagnosis codes, which may not have captured all the eligible patients. Moreover, images were acquired on multiple different PET scanners. Also, not all patients underwent CSF autoantibody testing. Lastly, the semiquantitative approach to image analysis suffers several limitations. The comparison group databases used by the Cortex ID software were small in number. The comparison database was also not optimized for younger age groups. Future prospective studies are needed with an increased number of encephalitis patients to fully determine different patterns of antibody-associated cortical metabolism.

CONCLUSION

We believe that brain ^{18}F-FDG PET/CT may serve as an important, early biomarker of AE. Current clinical recommendations do not include ^{18}F-FDG PET/CT in their algorithms, with MRI remaining the standard imaging modality. Our results in a small group of antibody-positive AE patients show a much greater sensitivity for detection of an underlying abnormality with ^{18}F-FDG PET/CT than with MRI. Because early intervention is paramount to optimal clinical outcome, our results suggest that ^{18}F-FDG PET/CT of the brain be added to the clinical workup of patients with suspected AE, particularly in those with normal or nonspecific MRI findings (*29*).

DISCLOSURE

No potential conflict of interest relevant to this article was reported.

REFERENCES

1. Linnoila JJ, Rosenfeld MR, Dalmau J. Neuronal surface antibody-mediated autoimmune encephalitis. *Semin Neurol.* 2014;34:458–466.
2. Lancaster E, Dalmau J. Neuronal autoantigens: pathogenesis, associated disorders and antibody testing. *Nat Rev Neurol.* 2012;8:380–390.
3. Wingfield T, McHugh C, Vas A, et al. Autoimmune encephalitis: a case series and comprehensive review of the literature. *QJM.* 2011;104:921–931.
4. Hughes EG, Peng X, Gleichman AJ, et al. Cellular and synaptic mechanisms of anti-NMDA receptor encephalitis. *J Neurosci.* 2010;30:5866–5875.
5. Mikasova L, De Rossi P, Bouchet D, et al. Disrupted surface cross-talk between NMDA and Ephrin-B2 receptors in anti-NMDA encephalitis. *Brain.* 2012;135:1606–1621.
6. Vitaliani R, Mason W, Ances B, Zwerdling T, Jiang Z, Dalmau J. Paraneoplastic encephalitis, psychiatric symptoms, and hypoventilation in ovarian teratoma. *Ann Neurol.* 2005;58:594–604.
7. Dalmau J, Tuzun E, Wu HY, et al. Paraneoplastic anti-N-methyl-D-aspartate receptor encephalitis associated with ovarian teratoma. *Ann Neurol.* 2007;61:25–36.

8. Braverman JA, Marcus C, Garg R. Anti-NMDA-receptor encephalitis: a neuropsychiatric syndrome associated with ovarian teratoma. *Gynecol Oncol Rep.* 2015;14:1–3.
9. Yanai S, Hashiguchi Y, Kasai M, et al. Early operative treatment of anti-N-methyl D-aspartate (anti-NMDA) receptor encephalitis in a patient with ovarian teratoma. *Clin Exp Obstet Gynecol.* 2015;42:819–821.
10. Alegre M, Dalmau J, Domingo P, Roe E, Alomar A. Successful treatment of major oral aphthous ulcers in HIV-1 infection after highly active antiretroviral therapy. *Int J Infect Dis.* 2007;11:278–279.
11. Lakhan SE, Caro M, Hadzimichalis N. NMDA receptor activity in neuropsychiatric disorders. *Front Psychiatry.* 2013;4:52.
12. Wang J, Wang K, Wu D, Liang H, Zheng X, Luo B. Extreme delta brush guides to the diagnosis of anti-NMDAR encephalitis. *J Neurol Sci.* 2015;353:81–83.
13. Veciana M, Becerra JL, Fossas P, et al. EEG extreme delta brush: an ictal pattern in patients with anti-NMDA receptor encephalitis. *Epilepsy Behav.* 2015;49:280–285.
14. Barry H, Byrne S, Barrett E, Murphy KC, Cotter DR. Anti-N-methyl-d-aspartate receptor encephalitis: review of clinical presentation, diagnosis and treatment. *BJPsych Bull.* 2015;39:19–23.
15. Iizuka T, Sakai F, Ide T, et al. Anti-NMDA receptor encephalitis in Japan: long-term outcome without tumor removal. *Neurology.* 2008;70:504–511.
16. Finke C, Kopp UA, Pruss H, Dalmau J, Wandinger KP, Ploner CJ. Cognitive deficits following anti-NMDA receptor encephalitis. *J Neurol Neurosurg Psychiatry.* 2012;83:195–198.
17. Graus F, Titulaer MJ, Balu R, et al. A clinical approach to diagnosis of autoimmune encephalitis. *Lancet Neurol.* 2016;15:391–404.
18. Mohr BC, Minoshima S. F-18 fluorodeoxyglucose PET/CT findings in a case of anti-NMDA receptor encephalitis. *Clin Nucl Med.* 2010;35:461–463.
19. Britton J. Autoimmune epilepsy. *Handb Clin Neurol.* 2016;133:219–245.
20. Trevino-Peinado C, Arbizu J, Irimia P, Riverol M, Martinez-Vila E. Monitoring the effect of immunotherapy in autoimmune limbic encephalitis using ^{18}F-FDG PET. *Clin Nucl Med.* 2015;40:e441–e443.
21. Park S, Choi H, Cheon GJ, Wook Kang K, Lee DS. ^{18}F-FDG PET/CT in anti-LGI1 encephalitis: initial and follow-up findings. *Clin Nucl Med.* 2015;40:156–158.
22. Kunze A, Drescher R, Kaiser K, Freesmeyer M, Witte OW, Axer H. Serial FDG PET/CT in autoimmune encephalitis with faciobrachial dystonic seizures. *Clin Nucl Med.* 2014;39:e436–e438.
23. Yuan J, Guan H, Zhou X, et al. Changing brain metabolism patterns in patients with ANMDARE: serial ^{18}F-FDG PET/CT findings. *Clin Nucl Med.* 2016;41:366–370.
24. Drzezga A, Grimmer T, Riemenschneider M, et al. Prediction of individual clinical outcome in MCI by means of genetic assessment and ^{18}F-FDG PET. *J Nucl Med.* 2005;46:1625–1632.
25. Singh TD, Josephs KA, Machulda MM, et al. Clinical, FDG and amyloid PET imaging in posterior cortical atrophy. *J Neurol.* 2015;262:1483–1492.
26. Thabane L, Mbuagbaw L, Zhang S, et al. A tutorial on sensitivity analyses in clinical trials: the what, why, when and how. *BMC Med Res Methodol.* 2013;13:92.
27. Titulaer MJ, McCracken L, Gabilondo I, et al. Treatment and prognostic factors for long-term outcome in patients with anti-NMDA receptor encephalitis: an observational cohort study. *Lancet Neurol.* 2013;12:157–165.
28. Zuliani L, Graus F, Giometto B, Bien C, Vincent A. Central nervous system neuronal surface antibody associated syndromes: review and guidelines for recognition. *J Neurol Neurosurg Psychiatry.* 2012;83:638–645.
29. Morbelli S, Djekidel M, Hesse S, Pagani M, Barthel H. Role of ^{18}F-FDG-PET imaging in the diagnosis of autoimmune encephalitis. *Lancet Neurol.* 2016;15:1009–1010.
30. Endres D, Perlov E, Stich O, et al. Hypoglutamatergic state is associated with reduced cerebral glucose metabolism in anti-NMDA receptor encephalitis: a case report. *BMC Psychiatry.* 2015;15:186.
31. Kojima G, Inaba M, Bruno MK. PET-positive extralimbic presentation of anti-glutamic acid decarboxylase antibody-associated encephalitis. *Epileptic Disord.* 2014;16:358–361.
32. Sekigawa M, Okumura A, Niijima S, Hayashi M, Tanaka K, Shimizu T. Autoimmune focal encephalitis shows marked hypermetabolism on positron emission tomography. *J Pediatr.* 2010;156:158–160.
33. Lee EM, Kang JK, Oh JS, Kim JS, Shin YW, Kim CY. ^{18}F-fluorodeoxyglucose positron-emission tomography findings with anti-N-methyl-D-aspartate receptor encephalitis that showed variable degrees of catatonia: three cases report. *J Epilepsy Res.* 2014;4:69–73.
34. Clapp AJ, Hunt CH, Johnson GB, Peller PJ. Semiquantitative analysis of brain metabolism in patients with paraneoplastic neurologic syndromes. *Clin Nucl Med.* 2013;38:241–247.
35. Irani SR, Michell AW, Lang B, et al. Faciobrachial dystonic seizures precede Lgi1 antibody limbic encephalitis. *Ann Neurol.* 2011;69:892–900.
36. Baumgartner A, Rauer S, Mader I, Meyer PT. Cerebral FDG-PET and MRI findings in autoimmune limbic encephalitis: correlation with autoantibody types. *J Neurol.* 2013;260:2744–2753.
37. Navarro V, Kas A, Apartis E, et al. Motor cortex and hippocampus are the two main cortical targets in LGI1-antibody encephalitis. *Brain.* 2016;139:1079–1093.
38. Sarria-Estrada S, Toledo M, Lorenzo-Bosquet C, et al. Neuroimaging in status epilepticus secondary to paraneoplastic autoimmune encephalitis. *Clin Radiol.* 2014;69:795–803.
39. Probasco JC, Benavides DR, Ciarallo A, et al. Electroencephalographic and fluorodeoxyglucose-positron emission tomography correlates in anti-N-methyl-d-aspartate receptor autoimmune encephalitis. *Epilepsy Behav Case Rep.* 2014;2:174–178.
40. Davis R, Dalmau J. Autoimmunity, seizures, and status epilepticus. *Epilepsia.* 2013;54(suppl 6):46–49.
41. Vernino S, Geschwind M, Boeve B. Autoimmune encephalopathies. *Neurologist.* 2007;13:140–147.
42. Dubey D, Sawhney A, Greenberg B, et al. The spectrum of autoimmune encephalopathies. *J Neuroimmunol.* 2015;287:93–97.
43. Alamowitch S, Graus F, Uchuya M, Rene R, Bescansa E, Delattre JY. Limbic encephalitis and small cell lung cancer: clinical and immunological features. *Brain.* 1997;120:923–928.
44. Dalmau J, Graus F, Villarejo A, et al. Clinical analysis of anti-Ma2-associated encephalitis. *Brain.* 2004;127:1831–1844.
45. Bosemani T, Huisman TA, Poretti A. Anti-Ma2-associated paraneoplastic encephalitis in a male adolescent with mediastinal seminoma. *Pediatr Neurol.* 2014;50:433–434.